



# Research on the Fire Behaviors of Polymeric Separator Materials PI, PPESK, and PVDF

Que Huang<sup>1,2,3</sup> , Xinxin Li<sup>2,3</sup>, Peijie Han<sup>4</sup>, Yang Li<sup>2,5</sup>, Changcheng Liu<sup>2,3</sup> , Qinpei Chen<sup>6,\*</sup> and Qiyue Li<sup>1,\*</sup>

<sup>1</sup> School of Resources and Safety Engineering, Central South University, Changsha 410010, China; que.huang@nuc.edu.cn

<sup>2</sup> School of Environment and Safety Engineering, North University of China, Taiyuan 030051, China; sz202214013@st.nuc.edu.cn (X.L.); liyangsafety@foxmail.com (Y.L.); ccliu@nuc.edu.cn (C.L.)

<sup>3</sup> Institute of Advanced Energy Materials and Systems, North University of China, Taiyuan 030051, China

<sup>4</sup> State Grid Shanxi Electric Power Corporation, Taiyuan 030001, China; hanpeijie@163.com

<sup>5</sup> School of Emergency Management and Safety Engineering, China University of Mining & Technology (Beijing), Beijing 100083, China

<sup>6</sup> Tianjin Fire Science and Technology Research Institute of MEM, Tianjin 300381, China

\* Correspondence: chenqinpei@ffri.com.cn (Q.C.); qyli@mail.csu.edu.cn (Q.L.)

**Abstract:** Certain polymers, such as polyvinylidene fluoride (PVDF), polyimide (PI), and poly(phthalazinone ether sulfone ketone) (PPESK), are commonly used separator materials in batteries. However, during the thermal runaway (TR) processing of batteries, significant heat is released by the combustion of the polymer separator. Therefore, analysis of the fire behaviors of polymer separator materials will facilitate a more comprehensive quantitative evaluation of battery thermal risk. This paper investigated the combustion properties of three types of polymers, namely, PVDF, PI, and PPESK, as potential separator materials by cone calorimetry and thermogravimetry (TG). A series of characteristic parameters, including ignition time (TTI), heat release rate (HRR), smoke production rate (SPR), and total heat release (THR), were evaluated for three polymers and blends (PI/PVDF, PPESK/PVDF) under an external heat flux of 45 or 60 kW/m<sup>2</sup>, respectively. The combustion characteristics and fire hazards of the three polymers and corresponding mixtures were analyzed through the comparative analysis of experimental data and phenomena. Under 60 kW/m<sup>2</sup>, the HRR curves of all polymers presented two peaks, while PI/PVDF and PPESK/PVDF mixtures exhibited one obvious peak. Moreover, the peak HRR (pHRR) for the mixed polymers was higher, indicating a relatively higher fire risk. However, in the application scenario, the mixed state represents the main polymer form as the active separator materials in batteries. The results showed that the specific coupling behaviors were related primarily to the component type. This work will help evaluate the fire risk of polymeric separator materials based on the combustion characteristics to predict the safety of mixtures in batteries and develop new methods for fire suppression.

**Keywords:** polymer; thermogravimetric analysis; cone calorimetry; combustion characteristics; safety



**Citation:** Huang, Q.; Li, X.; Han, P.; Li, Y.; Liu, C.; Chen, Q.; Li, Q. Research on the Fire Behaviors of Polymeric Separator Materials PI, PPESK, and PVDF. *Fire* **2023**, *6*, 386. <https://doi.org/10.3390/fire6100386>

Academic Editor: Qingsong Wang

Received: 21 July 2023

Revised: 1 October 2023

Accepted: 6 October 2023

Published: 8 October 2023



**Copyright:** © 2023 by the authors. Licensee MDPI, Basel, Switzerland. This article is an open access article distributed under the terms and conditions of the Creative Commons Attribution (CC BY) license (<https://creativecommons.org/licenses/by/4.0/>).

## 1. Introduction

Lithium-ion batteries (LIBs) have been produced for decades. Due to their high energy density, long cycle life, high power, and environmental protection, LIBs are widely used in laptops, smartphones, digital cameras, and other portable electronic products associated with 3C (computer, communication, and consumer electronics). LIBs comprise four core parts: positive electrode, negative electrode, separator, and electrolyte. The battery separator has an important role as it is inextricably associated with battery safety. However, since the advent of LIBs, battery explosion or combustion accidents have occurred almost yearly; the fundamental problem is their thermal safety [1]. The main causes of LIB thermal runaway (TR) are mechanical, electrical, and thermal abuse, all of which are associated with internal short circuits (ISCs); hence, the separator becomes damaged, causing the positive

and negative electrodes to be in direct contact, releasing a significant amount of heat. The main causes of ISCs are separator defects, including age-associated rupture, buildup of metal dendrites, a pierced separator caused by external force extrusion, or shrinking and melting of the separator caused by overheating [2]. Therefore, selecting novel separator materials with good mechanical properties and high thermal stability can reduce the risk of ISC and TR of the battery, improving safety.

To meet the demand of the current working environment for LIBs, various new composite separator materials have been developed and optimized in terms of preparation process improvement. Among them, polyvinylidene fluoride (PVDF) has been widely used as a binder and coating material in LIBs due to its good mechanical strength, superior chemical/electrochemical/thermal stability, and excellent affinity for electrolytes. In addition, polyimide (PI) shows excellent heat resistance, chemical stability, good mechanical performance, and extremely high electrical insulation properties, potentially due to the special engineered plastics, high-performance fibers, selective membranes, high-temperature coatings, and composite materials. Therefore, PI-related materials are well suited for use as safe battery separators with high temperature resistance. However, recently, a blended PI nanofiber battery separator was developed by high-voltage electrostatic blending and high-temperature imide treatment of two precursors. This battery contains a PI precursor that does not melt at high temperatures and one that melts at 300–400 °C. Hence, it exhibits high-temperature resistance, chemical stability, and porosity, as well as good mechanical strength and permeability [3]. Liang et al. [4] studied a separator with a porous layer, high thermal resistance, convenient operation, and high PI proportion that improved LIB safety. Additionally, a polymer separator obtained by compounding poly(aryl ether) with thermoplastic resin has received extensive attention due to its superior electrical conductivity and high safety [5–7]. Lu et al. [8] and Gong et al. [9] prepared a series of poly(aryl ether) materials by introducing phthalazinone, including poly(phenylene ether ketone) (PPEK), poly(phthalazinone ether sulfone) (PPES), poly(phthalazinone ether sulfone ketone) (PPESK), etc.; the materials' glass transition temperature exceeded 533 K and the 5% weight loss temperature was ~773 K. Moreover, the synthesized separators comprising these materials and PVDF generated via electrospinning exhibited excellent electrochemical performance and thermal stability. A novel PPESK/PVDF/PPESK composite interlayer separator for LIBs was proposed to be synthesized by electrospinning and predicted to have good thermal dimensional stability and thermal self-closing performance to prevent ISC. Hence, the fire risk of LIBs can be quantitatively evaluated by determining the pyrolysis mechanism, combustion characteristics of polymer separator materials, and their effects on TR.

The study of combustion characteristics is interdisciplinary, covering combustion, turbulence, radiation, and material science, all of which have equally important roles. Therefore, evaluation of the polymer separator combustion behavior is a complex challenge. More specifically, the physical and chemical properties of the material must be considered, as well as the effects of different heat sources, transfer mechanisms, and changes in the combustion environment, such as temperature, humidity, oxygen concentration, or airflow. Additionally, the decomposition behavior of polymer materials depends largely on the environment in which they begin to decompose [10], particularly the external heat flux [11]. To date, more than 37 methods are employed to characterize the combustion characteristics, including the limiting oxygen index (LOI) method [12], horizontal and vertical combustion method, smokebox method put forward by the National Bureau of Standards (NBS) to measure smoke density, and tunnel method to measure flame propagation velocity. To evaluate the combustion characteristics of polymer materials more comprehensively, a cone calorimeter was invented in 1982 to study the heat release of materials under certain heat flux [13]. That is, after the sample is placed under a conical cover with a preset heat flux, the parameters, such as heat release rate (HRR), smoke production rate (SPR), and total heat release (THR), are calculated by the established program to characterize the combustion behavior of the material. The environment is similar to the real fire environment, which can

more accurately characterize the combustion characteristics of the polymer. Indeed, it has particular reference value in evaluating, designing materials, and evaluating fire risk [14].

The principle of cone calorimetry is based on oxygen consumption (OC); for every 1 kg of oxygen consumed, the heat released is approximately 13.1 kJ/g, and the deviation of OC and combustion heat between polymer materials is 5%. The heat release amount of the burning substance can be calculated according to O<sub>2</sub> combustion. According to previous studies, HRR is one of the most important variables in determining fire risk [15]. In all fires, most casualties are caused by smoke poisoning, followed by burns and suffocation; hence, analysis of smoke products produced by thermoplastic polymer combustion is essential [16]. Thermogravimetry (TG) is also a commonly used method to determine the thermal stability of polymers quantitatively. Thermogravimetric analysis (TGA) could be applied to measure the relationship between the mass and temperature of the polymer separator to evaluate the material's thermal stability under pre-setting the starting, heating, and cutoff temperature conditions in the program [17]. It can also be used to analyze the kinetics of polymer thermal decomposition. When comparing the thermal stability of different polymer materials, the mass loss percentage is generally used for comparative analysis. Through the comparative analysis of the polymer material mass loss and temperature, insights are obtained regarding the relationship between the thermal stability and mass of the polymer and intermediate products produced during the thermal decomposition process. In addition, many factors influence the TGA, including differences between the experimental conditions and different samples. Hence, to increase the accuracy and repeatability of the thermogravimetric curve, it is necessary to analyze various influencing factors before the experiments and determine the heating rate, start and end temperatures, air flow rate, and other parameters. The heating rate of the TGA is generally controlled in the range of 5 to 20 K/min. Typically, the lower the heating rate of the test sample, the higher the resolution. When TGA is carried out on polymer materials, the polymer's properties inevitably change due to residual solvents or historical effects. In this case, repeated experiments can generally eliminate errors [18].

Hermouet et al. [10] studied the effect of local oxygen concentration on polymer combustion using a cone calorimeter with a controlled atmosphere. Regarding the fire spread of organic polymer materials, the heat transfer mechanism primarily includes flame heat feedback, convection, and heat conduction inside the fuel. Based on heat transfer analysis and relevant experiments, worldwide, prediction models of fire spread rate have been established under different conditions of external heat flux, dip angle, and flow rate [19,20]. In addition, Parthasarathy et al. [21] used the thermogravimetric method to analyze the stability of organics and the Flynn-Wall-Ozawa model to calculate the thermodynamic properties of reactions. Meanwhile, Zheng et al. [22,23] carried out numerical simulation analysis on the fire spread behaviors of polymethyl methacrylate (PMMA), and constructed a melting model to determine the influence of dimensionless parameters on the fire spread behaviors. Kim et al. [24] simulated the melting dripping behaviors of polypropylene (PP) under external radiation and simplified many influencing factors in the simulation process. Additionally, Wen et al. [25] simulated the melting dripping of flame retardant polyethylene (PE); the results showed that the carbon particle additives could effectively reduce the dripping rate. These previous studies validate that the present study is meaningful to some extent for the safety evaluation of polymers. However, many scholars are also concerned about the effects of air humidity and moisture on polymer combustion properties. Although the research on polymers has been relatively sufficient, in a real fire, the combustibles do not typically comprise only polymers, making it necessary to evaluate the combustion behavior of the mixed polymer phase and assess the fire risk of polymers in a mixed state.

Overall, the separator is the LIB component with the highest heat release per unit mass; thus, it is of considerable importance to evaluate the pyrolysis mechanism and combustion characteristics of the separator to evaluate the fire risk of LIBs quantitatively. However, the complexity of the chemical structures of PVDF, PI, and PPESK as raw materials of the new composite separator complicates these analyses. Accordingly, the current study analyzes

the kinetic characteristics of PVDF, PI, PPESK, PI/PVDF, and PPESK/PVDF to supplement the quantitative evaluation of battery safety. Importantly, this is the first study to apply cone calorimetry to investigate these substances. Moreover, the thermal decomposition processing of the polymer separator was evaluated, the mechanism function was assessed, and the kinetic parameters were solved. The influence of external heat flux and other key factors on the distribution of gaseous products was further studied to provide insights regarding the sample dissociation path and primitive reaction. The combustion behaviors of the samples were then examined, and the proportion of the thermal release was calculated. In this way, the thermal decomposition behaviors of separator materials, including PVDF, PI, PPESK, and their mixed phase, are evaluated and compared by analyzing the combustion characteristics of the three polymer compounds at a certain ratio. Additionally, the effect of external heat flux on the combustion process was determined. Finally, the HRR, SPR, ignition time (TTI), and THR under different heat fluxes were characterized by cone calorimetry and TG. Collectively, the results of this study broaden the understanding of polymer separator safety and clarify the role of the separator in the TR behaviors of LIBs.

## 2. Experiments

### 2.1. Experimental Materials

PVDF and PI powders were provided by Dongguan Zhanyang Polymer Materials Co., Ltd. (Dongguan, China) and Nanjing Quanxi Chemical Co., Ltd. (Nanjing, China), respectively. PPESK, in a sawdust state, was supplied by Suzhou Jiahui Company (Suzhou, China). The average molecular weight (MW) of PVDF is approximately 400,000, with a PI of approximately 44,000. The category of PI applied in this study is aromatic, with an imide ring in the main chain, which is rigid and insoluble and is used primarily as membranes or solid powders. The molar ratio of PI to PVDF in the PI/PVDF mixture was 1:1 based on MW, and of PPESK to PVDF in PPESK/PVDF was 1:1 based on the relative molar mass of the PPESK/PVDF separator. These ratios were selected based on the proportion of each polymer in the composite separator of LIBs. PI/PVDF and PPESK/PVDF were mixed in a ball mill for at least one minute to guarantee homogeneous mixing; there were no chemical reactions between the samples and components. No solvent was added during the mixing process; thus, no drying step was required. According to the International Organization for Standardization (ISO) 5660-1 “Reaction-to-fire tests—Heat release, smoke production, and mass loss rate—Part 1: Heat release rate (cone calorimeter method) and smoke production rate (dynamic measurement)” standard [13], the final physical state of the samples was powder. The samples were weighed by an electronic scale with an accuracy of 0.01 g; the densities are listed in Table 1.

**Table 1.** Density of polymer samples used in this work.

Sample	Density (g/cm <sup>3</sup> )
PI	1.43
PPESK	1.37
PVDF	1.78
PPESK/PVDF	1.26
PI/PVDF	1.31

### 2.2. Experimental Instruments

A cone calorimeter (PX-07-007, produced by Suzhou Phoenix Instrument Co., Ltd., Suzhou, China) was applied to detect the fire parameters, comprising six parts: ventilation device, combustion chamber, lifting platform, smoke measurement system, oxygen analyzer, and related auxiliary equipment (Figure 1). The data acquisition system was manufactured by Nanjing Jiangning Analytical Instrument Co., Ltd., Nanjing, China, and

the thermogravimetric analyzer was purchased from Mettler-Toledo International Inc., Columbus, OH, USA.

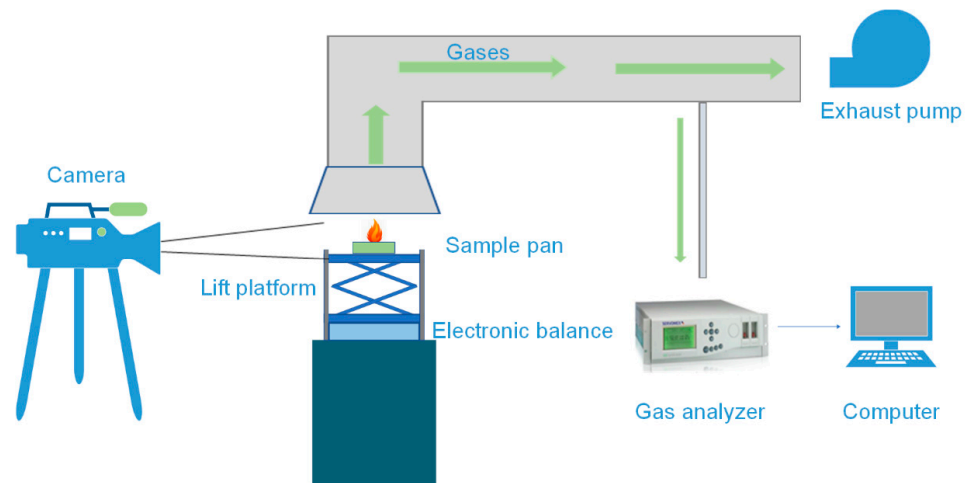


**Figure 1.** Principle diagram of the used cone calorimeter.

### 2.3. Experimental Methods

The cone calorimeter experiments were carried out according to the ISO 5660-1 “Reaction-to-fire tests—Heat release, smoke production and mass loss rate—Part 1: Heat release rate (cone calorimeter method) and smoke production rate (dynamic measurement)” standard [13]. For each measurement, 10 g of sample was weighed in advance and placed in a 5 cm × 5 cm metal pan wrapped in aluminum foil, and the appropriate height was adjusted. Aluminum foil was applied according to ISO-5660 so that only the upper surface of the sample would receive radiation, which is a common practice in cone calorimeter testing to avoid the thermal heat flux from the sample tray/pan, holder, etc., and improve the accuracy of the results. The electronic balance was placed under the lifting frame and returned to zero. The characterization experiments were performed at a heat flux of 30, 45, or 60 kW/m<sup>2</sup>. At 30 kW/m<sup>2</sup>, the signal given by the instrument was consistently low, and the background noise was relatively high, preventing accurate analysis; hence, only the results at 45 and 60 kW/m<sup>2</sup> were analyzed in most cases. Three thermocouples were set on the surface of the material above the sample pan (regarded as 0 cm) and at 1 cm and 2 cm from the surface to collect data through an Agilent 34970A data acquisition device (Agilent Technologies, Inc., Santa Clara, CA, USA). The system automatically started the test after collecting baseline results for 60 s. During the test, the ignition and fire extinguishing time and the beginning and ending of the smoke time were recorded. A camera recorded the entire process to analyze the combustion phenomena. The test was completed at the end of the smoldering, surface combustion, or flaming combustion. After the test, the initial and remaining sample mass, HRR, smoke release rate, and other data were saved in the corresponding folders.

TGA was performed using a thermogravimetric analyzer, and the measurements were performed in an N<sub>2</sub> atmosphere. The primary function of N<sub>2</sub> was to prevent the oxidation of the instrument. The gas flow rate was set to 50 mL/min, and the temperature increased from 303 to 1073 K with a heating rate of 20 K/min. A ceramic crucible was used in the tests. First, the initial test temperature was set at 303 K. Next, an empty crucible was used for firing, and the blank experiment was conducted as a baseline to reduce the measurement error. Subsequently, 3 mg of each sample was placed in the crucible to select the set procedure for the experiment. The detection was stopped after the mass of the sample to be tested was ~0, it was no longer reduced, or the curve plateaued for a certain period; the experimental data was saved after normalization.

According to the cone calorimeter test standard, each experiment was repeated at least twice to guarantee reproducibility. The average value from the duplicate samples was taken for analysis. Data will be made available upon request.

#### 2.4. Calculation Methods

##### 2.4.1. Heat Release Rate

HRR refers to the rate of heat release during the combustion reactions of polymer materials in per unit area at per unit time, which is one of the most important parameters used to quantify the fire risk of flammable substances. The value was calculated according to Equation (1):

$$\dot{q}(t) = \left( \frac{\Delta h_c}{r_0} \right) (1.10) C \sqrt{\frac{\Delta p}{T_e}} \cdot \frac{x_{O_2}^0 - x_{O_2}}{1.105 - 1.5x_{O_2}} \quad (1)$$

where  $\frac{\Delta h_c}{r_0}$  is an empirical constant as  $13.1 \times 10^3$  kJ/kg;

$C$  is the calibration constant of the orifice flowmeter;

$\Delta p$  is the pressure difference of the orifice flowmeter;

$T_e$  is the absolute temperature of the gas on the orifice flowmeter;

$x_{O_2}^0$  is the average value of the oxygen mole fraction measured during the 1-min baseline measurement;

$x_{O_2}$  is the molar fraction of oxygen measured by the oxygen analyzer.

As a rule, the higher the HRR, the shorter the ignition time, the greater the risk of fire.

##### 2.4.2. Fire Performance Index

The fire performance index (FPI) was expressed as per Equation (2):

$$FPI = \frac{TTI}{pHRR} \quad (2)$$

where  $FPI$  represents the fire hazard during material combustion,  $(m^2 \cdot s)/kW$ .

$pHRR$ ,  $kW/m^2$ .

$TTI$ , s.

##### 2.4.3. Fire Growth Index

The fire growth index (FGI), was calculated using Equation (3):

$$FGI = \frac{pHRR}{Time\ to\ pHRR} \quad (3)$$

where  $FGI$ ,  $kW/(m^2 \cdot s)$ .

$pHRR$ ,  $kW/m^2$ .

$Time\ to\ pHRR$ , s.

##### 2.4.4. Broido Method to Achieve Activation Energy from Thermogravimetry

To calculate the activation energy of the polymer materials, the Broido method [26] was applied, expressed by Equation (4):

$$y = \frac{(W_t - W_\infty)}{(W_0 - W_\infty)} \quad (4)$$

where  $W_t$  is the weight of the sample at any time, s.

$W_0$  is the initial weight of the sample, g.

$W_\infty$  is the final residue mass of the sample, g.

The reaction rate was calculated as derived in Equation (5):

$$\frac{dy}{dt} = -ky^n \quad (5)$$

where  $k$  is the specific rate constant. In this case, the reaction order  $n$  is 1. Thus, Equation (5) was simplified to Equation (6):

$$\frac{dy}{dt} = -ky \quad (6)$$

When the rate constant  $k$  varied with temperature, the Arrhenius Equation (7) was used:

$$k = Ae^{-\frac{E_a}{RT}} \quad (7)$$

where  $k$  is the rate constant at temperature  $T$ ;

$A$  is the pre-exponential factor, also known as Arrhenius constant;

$e$  is the base of the natural logarithm.

$E_a$  is the experimental activation energy, which can be generally regarded as a constant independent of temperature, kJ/mol;

$R$  is the molar gas constant, J/(mol·K);

$T$  is the absolute temperature, K.

Substituting Equation (7) into Equation (6), considering the heating rate in TG [26], Equation (8) was obtained:

$$\frac{dy}{y} = -\left(\frac{A}{u}\right)e^{-\frac{E_a}{RT}} \cdot dT \quad (8)$$

where  $u$  is the heating rate, K/s.

By integrating both sides, Equation (9) was created:

$$\int_y^1 \frac{dy}{y} = \frac{A}{u} \int_{T_0}^T e^{-\frac{E_a}{RT}} \cdot dT \quad (9)$$

Many pyrolysis processes can be represented as first order reactions, as represented by Equation (10):

$$\int_y^1 \frac{dy}{y} = -\ln y = \ln\left(\frac{1}{y}\right) \quad (10)$$

By combining Equations (9) and (10), the logarithm was obtained from integration, as depicted in Equation (11):

$$\ln\left(\ln\left(\frac{1}{y}\right)\right) = \frac{E_a}{RT} + Constant \quad (11)$$

From Equation (11), by taking the  $\ln\left(\ln\left(\frac{1}{y}\right)\right)$  as the ordinate and  $\frac{1000}{T}$  as the abscissa, the activation energy  $E_a$  of the polymer reactions was calculated.

### 3. Results and Discussion

#### 3.1. Experimental Phenomena and Smoke/Ignition Time

TTI is considered an important parameter in characterizing the fire hazard and thermal decomposition degree of materials. Generally, samples with low TTI have higher fire risk. Many theories and models have been proposed based on the TTI, incident radiation, and physical properties of the material for TTI analysis. Hence, the study of TTI has considerable importance [27,28].

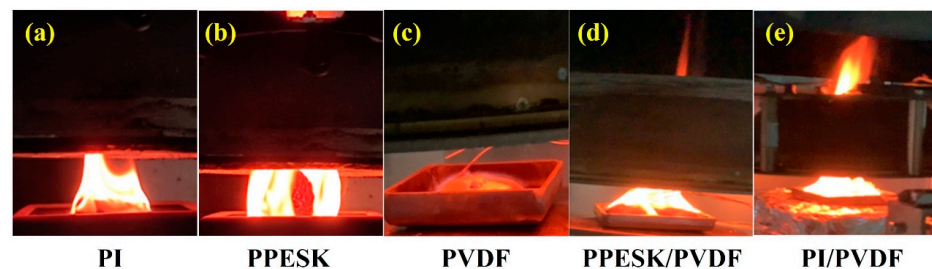
As PVDF, PI, and PPESK are polymers with extremely high thermal stability, only PI burned under the external heat flux of 45 kW/m<sup>2</sup> based on the combustion phenomena. Therefore, all polymers were characterized by smoke/ignition time at heat flux of/above 45 kW/m<sup>2</sup>, as presented in Table 2.

**Table 2.** Experimental phenomena and smoke/ignition time of samples under 45 and 60 kW/m<sup>2</sup>.

Heat Flux	Experimental Phenomena and Smoke/Ignition Time									
	PVDF		PI		PPESK		PI/PVDF		PPESK/PVDF	
45 kW/m <sup>2</sup>	fume 37 s	extinction 357 s	fume 87 s	extinction 554 s	fume 301 s	extinction 1200 s	fume 60 s	extinction 435 s	fume 70 s	extinction 520 s
60 kW/m <sup>2</sup>	ignition 240 s	extinction 1300 s	ignition 107 s	extinction 1906 s	ignition 166 s	extinction 1800 s	ignition 405 s	extinction 1700 s	ignition 234 s	extinction 1142 s

From the time data and corresponding phenomena, PI had the shortest ignition time, and PVDF had the longest under the same heat flux. However, the burning period of PI was the longest, while that of PPESK was the shortest. In the mixed state, the TTI and continuous combustion time of the polymer mixture was between that of the two macromolecular polymer types, indicating that the polymer separator with a low ignition point would burn first, igniting the material with the high ignition point and increasing the fire risk.

Flammable combustion refers to combustible materials being ignited and continuing to burn after removing the ignition source under specified experimental conditions. Meanwhile, surface combustion refers to the flameless combustion phenomenon occurring on the surface of the material due to the direct reaction between combustible solids and oxygen. Figure 2 shows that the combustion phenomenon of pure PVDF was considered surface combustion, while PI exhibited relatively weak flame combustion without apparent volume expansion. In contrast, PPESK presented violent flammable combustion, and its volume changed markedly after heating. This was due to the thermal decomposition reactions of thermoplastic materials occurring at the material's surface and in deeper layers. When the temperature increased, the chemical bonds began to break, and the MW and viscosity of the polymer decreased, resulting in melting. However, the gases would not immediately overflow from the surface; rather, gases would accumulate until the surface of the polymer was broken by high-temperature volatiles [29,30]. After the polymer was mixed at a certain proportion, the combustion phenomenon would become more violent than that of a single polymer. In particular, under the combination of PI/PVDF, a dynamic jet flame was observed with a height that surpassed that of the other groups. Meanwhile, the combustion of PPESK/PVDF was weaker than that of PI/PVDF, however it was more intense than the single polymers. This may have resulted from the diffusion rate of oxygen in the polymer being much slower than the cracking rate of the polymer when the ignition temperature exceeded 573 K. The polymer with a lower ignition point was first ignited, and the heat conduction rate was much faster than the heat flux, causing the polymer with a higher ignition point to ignite and the fire scale to increase. This was confirmed by the recorded phenomena and data presented in Table 2.

**Figure 2.** Combustion phenomena of different polymer materials as (a) PI, (b) PPESK, (c) PVDF, (d) PPESK/PVDF and (e) PI/PVDF under a heat flux of 60 kW/m<sup>2</sup>.



### 3.2. Heat Release Rate

The HRR curves of the polymer separator materials under a heat flux of 45 and 60 kW/m<sup>2</sup> are presented in Figure 3. Under 45 kW/m<sup>2</sup>, signals were not apparent (Figure 3a). The three polymers had two obvious peaks, followed by a long step (Figure 3b), which might be due to the different combustion order of the pyrolysis substances [31,32]. It was speculated that due to the temperature increase in the materials after heating, the thermal decomposition reactions produced different volatile combustible gases, which ignited. Since the pyrolysis products of the polymers varied at different temperatures, their contributions to the peaks also differed, causing the appearance of different peaks. With the increase in combustible gases generated by the thermal decomposition reactions, the HRR peaked and began to decline due to the decrease in the combustible gases generated by the reactions. Alternatively, the polymers may have formed a relatively dense heat-resistant outer surface with the development of pyrolysis during combustion; the thermal decomposition reactions of the polymers could have then occurred at a certain thickness [33]. That is, the thermal decomposition reactions would also occur inside the polymers. As the temperature continued to rise, the dense heat-resistant outer surface cracked and released the volatile combustible gases inside the polymers. Due to the gradual expansion of the cracks, the second peak value of HRR (pHRR) emerged. However, theoretical studies have suggested that the second peak might have been due to heat transfer to the back of the thermal insulation material [34–36] and the accumulation of energy generated by the insulation, resulting in increased HRR. However, regarding the PI/PVDF and PPESK/PVDF mixtures, only one peak was observed, which was postulated to be due to the relatively flammable polymer component igniting the other polymer, triggering positive feedback in the mixed system. The temperature then rapidly increased, and all materials were ignited instantaneously, resulting in only one apparent peak.

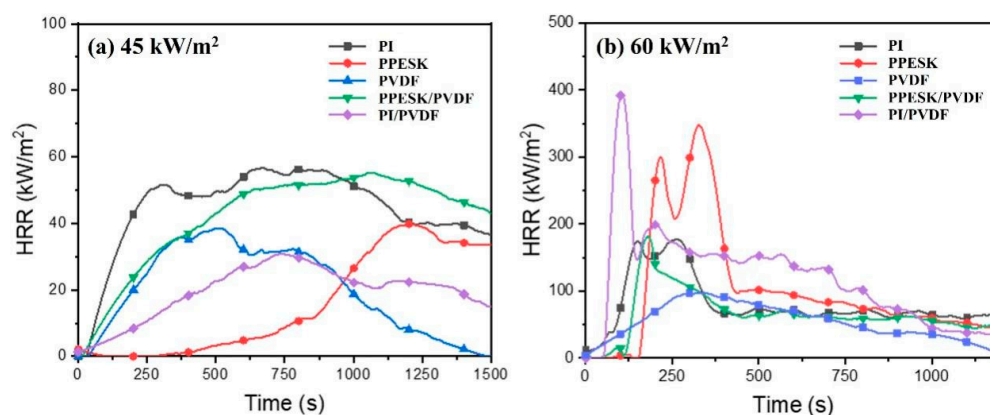


**Figure 3.** HRR curves of polymer separator materials under a heat flux of (a) 45 and (b) 60 kW/m<sup>2</sup>.

Besides the highest point in the HRR curve being designated the pHRR, THR is also important for characterizing the combustion characteristics of polymer materials. More specifically, they reflect the most intense heat release of polymer combustion and the sum of heat generated during the combustion process, respectively, making them important variables in determining the risk of polymer fire. At a heat flux of 45 kW/m<sup>2</sup>, the pHRR of all single polymers and mixtures was similar as no flame burning occurred for PDVF, PPESK, PI/PVDF, or PPESK/PVDF; meanwhile, PI presented weak flame combustion (Figure 4). Flame combustion occurred in all samples under the 60 kW/m<sup>2</sup> heat flux, and the fire safety could be more intuitively characterized and analyzed. At 60 kW/m<sup>2</sup>, the trend in pHRR and THR was consistent across the samples. The highest peak for the single polymers was generated during PPESK combustion. Hence, the pHRR of the PPESK/PVDF mixture was approximately 76.1% higher than that of PVDF and approximately 25.2% lower than that of PPESK. The THR order was also PPESK > PPESK/PVDF > PVDF. In

contrast, the pHRR of the PI/PVDF mixture was 239.3% and 991.1% higher than that of PI or PVDF, respectively. Although the THR was also higher for the mixture than that of the two polymers, the increase was not as sharp as that of pHRR. Therefore, the combustion characteristics of the mixtures were relatively complex. In addition, the greater the external heat flux, the higher the pHRR and THR, and the more serious the fire risk of the polymer separator.

In summary, the polymer fire is more prone to smoke poisoning in the early stage of the fire and will develop to suffocation in the middle and late stages. In addition, PVDF generated a large amount of CO in the 250–750 s period, indicating that PVDF had a long incomplete combustion stage, resulting in highly toxic CO production (Figure 5b). According to Figure 5a–c, the smoke production by PPESK remained high after 500 s, while CO and CO<sub>2</sub> production was low, indicating that PPESK tended to generate solid products, such as soot particles, and low levels of gas products during combustion.

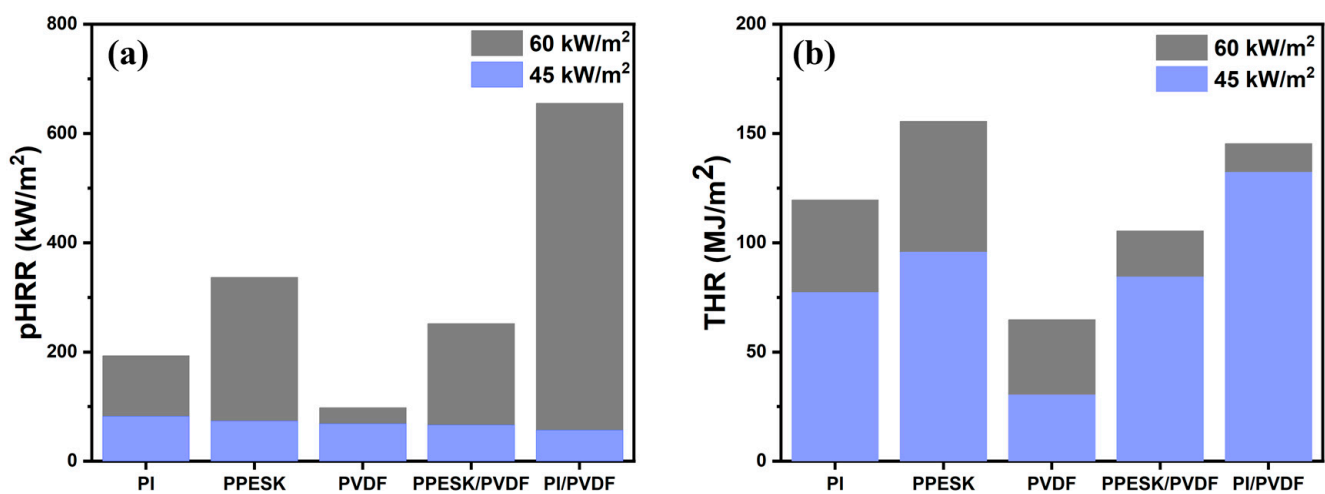
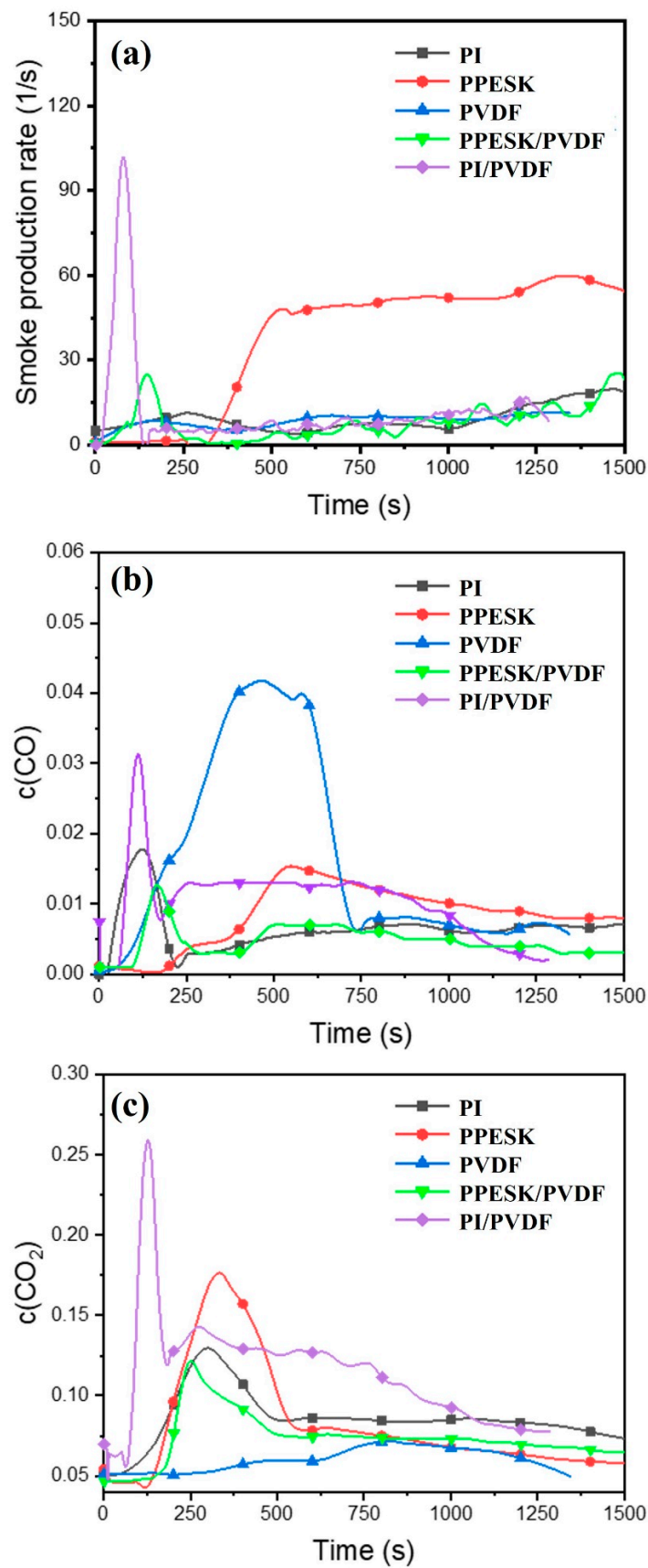


Figure 4. (a) pHRR and (b) THR of different polymers under heat fluxes of 45 and 60 kW/m<sup>2</sup>.

### 3.3. Flue Gas Analysis

Typically, when a fire occurs, the key factors causing the largest casualties are the shielding effect of smoke and its toxicity, however, polymer materials are a primary source of fire smoke. The gases produced in the fire mainly comprise CO and CO<sub>2</sub>. Thus, measuring the smoke release rate of polymer materials and the concentration changes of various gases is necessary. The gas analyzer in this study was sampled from the exhaust pipe, which could directly analyze and quantify CO, CO<sub>2</sub>, and O<sub>2</sub>. As indicated in Figure 5a, when the materials were in flame combustion or smoldering, surface combustion processing, their gas production and flue gas product types differed significantly. As presented in Figure 5b,c, the fitting degree of CO<sub>2</sub> content and HRR curves was high, while that of CO concentration and the HRR curve was not. Therefore, it was speculated that the polymer materials released a large amount of CO<sub>2</sub> when burning, and the total amount of flue gas markedly increased. The CO content produced by the polymer materials during smoldering was significantly greater than that of flame or surface combustion. The only group with CO concentration changes that were to the HRR curve was PI/PVDF. This might have been due to the intense combustion phenomenon of PI/PVDF. The amount of O<sub>2</sub> in the air was insufficient to maintain the complete combustion of PI/PVDF, resulting in more CO being produced.



**Figure 5.** (a) SPR and relative values of (b) CO and (c) CO<sub>2</sub> concentrations from different polymer flue gases.

### 3.4. Combustibility Index

To perform a more comprehensive analysis of the fire risk of each material, the data measured by the cone calorimetry method can be statistically integrated. This has led to the proposal of several comprehensive evaluation indicators that provide a more intuitive representation of the combustion behaviors of various materials [27,28].

#### 3.4.1. Fire Performance Index

The longer ignition time and lower pHRR would increase FPI, indicating that the material is not readily ignited after heating. In this case, the flashover phenomenon would not easily occur, and thus, the fire risk would not be high. Contrarily, a low FPI indicates that the material is readily ignited and dangerous, as FPI is an attribute of the material.

#### 3.4.2. Fire Growth Index

The less time required to reach pHRR and the greater the pHRR, the higher the FGI, indicating that the fire will spread rapidly after the combustion of the material, and the fire risk would also increase. In contrast, a low FGI indicates that the fire growth is relatively slow and the fire risk is not high.

The FPI and FGI of the five samples were calculated according to Equations (2) and (3) and are presented in Table 3.

**Table 3.** Combustion characteristic index of polymer separator materials under 60 kW/m<sup>2</sup>.

Heat Flux	Index Type	PI	PPESK	PVDF	PPESK/PVDF	PI/PVDF
60 kW/m <sup>2</sup>	FPI (dimensionless parameter)	0.56	0.50	2.5	0.53	0.62
	FGI (dimensionless parameter)	0.72	1.05	0.36	1.57	6.90

From the values listed in Table 3, it is apparent that the fire risk of the polymer materials varied greatly. In general, the higher the FPI, the lower the FGI, the better the flame retardant properties of the material. As a result, the fire risk of PPESK was the largest among the three macromolecular polymers, followed by PI and PVDF. Under a heat flux of 60 kW/m<sup>2</sup>, the FPI of PI was ~12.0% higher than that of PPESK but only accounted for 22.4% that of PVDF. From the perspective of FGI, that of PI was 31.4% lower than that of PPESK and twice that of PVDF. As for the mixtures, the fire risk indexes of PPESK/PVDF were slightly higher than those of PPESK. However, the comprehensive fire risk of PI/PVDF was considerably higher than that of PI and PVDF. The FGI was 858.3% higher for PI/PVDF than PI, indicating that the combination of PI and PVDF would rapidly increase the thermal hazard. Notably, after the mixture of polymers, the fire risk has a high probability of increasing to a certain extent.

### 3.5. Thermogravimetric Analysis

TGA can be divided into isothermal processing [37] and non-isothermal processing [38]. However, it is difficult to achieve ideal isothermal conditions. Therefore, the non-isothermal method is often used to analyze the thermal decomposition of substances. Using TGA, the thermal stability of the various polymer materials was compared, and the pyrolysis behaviors of the polymers under heat action were analyzed [39–42]. The thermal decomposition reactions of materials depend on several factors, including polymer type, mass, and particle size. The polymer materials used in this study were all powdered, and the mass of each sample was controlled. The kinetic parameter of activation energy ( $E_a$ ) in the thermal degradation process was calculated by the Broido method [26], and the difficulty level of releasing energy during combustion of the polymer separators was quantitatively analyzed according to the activation energy required for the reactions. Thermal degradation includes kinetics, thermodynamics, and a reaction mechanism, which is a

complicated process that depends on the temperature, sample state, placement form, and time. Although TGA cannot be used to display products of polymer materials visually, it can provide significant insights for the safety evaluation of polymer separators and explanations of combustion phenomena.

Figure 6 and Table 4 show that the thermogravimetric curves of various polymer samples exhibited apparent stages, and those of mixed polymers had a higher consistency than those of single polymers. According to the slopes, the TG results of mixtures resulted from the positive feedback between two single polymer substances during the combustion process.

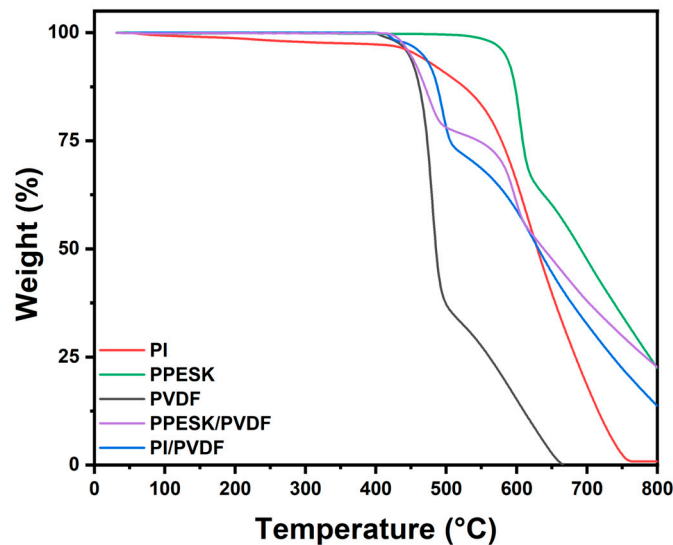


Figure 6. Thermogravimetric curves of different polymer materials.

Table 4. Mass loss percentage of each sample at different temperatures using TGA.

Sample	Temperature				
	600 K	700 K	800 K	900 K	1000 K
PVDF	0%	1%	68%	92%	100%
PI	2.4%	3%	13%	46%	91%
PPESK	0%	0%	1%	35%	58%
PPESK/PVDF	0%	1%	24%	46%	66%
PI/PVDF	0%	1%	18%	46%	73%

Through Equations (4)–(11), the activation energy of the polymer reactions were calculated using the slope fitting function in Origin 2022 software, as presented in Table 5.

A higher activation energy indicates that the reaction requires more energy. When the required temperature is relatively high, a slight change in the temperature has little effect on the reaction. Conversely, when the required activation energy is lower, a slight change in the temperature can greatly impact the chemical reaction. From Table 5, it can be concluded that PI required the least energy in the first stage, suggesting that PI was most likely to start the reaction, while PPESK required the most energy in Step 1. However, the activation energies required for the second stage for all three polymers were much lower than those of the first stage. According to the TGA of the polymer mixtures, the activation energy of the first stage for each blend was lower than that of the components in the same step. Hence, the separator materials would be more likely to burn after mixing, increasing the fire risk of the polymer mixtures.

**Table 5.** Kinetic parameters of different polymers from TGA.

Polymer Material	Pyrolysis Stage	The Starting Temperature of Pyrolysis Stage	Activation Energy
PVDF	Step 1	679 K	$30.83 \pm 0.33$ kJ/mol
	Step 2	770 K	$6.64 \pm 0.21$ kJ/mol
PI	Step 1	765 K	$27.88 \pm 0.05$ kJ/mol
	Step 2	830 K	$13.67 \pm 0.15$ kJ/mol
PPESK	Step 1	836 K	$42.37 \pm 0.65$ kJ/mol
	Step 2	891 K	$10.10 \pm 0.16$ kJ/mol
PPESK/PVDF	Step 1	702 K	$26.05 \pm 0.69$ kJ/mol
	Step 2	767 K	$2.68 \pm 0.05$ kJ/mol
	Step 3	844 K	$13.70 \pm 0.24$ kJ/mol
	Step 4	883 K	$7.74 \pm 0.12$ kJ/mol
PI/PVDF	Step 1	691 K	$19.82 \pm 0.42$ kJ/mol
	Step 2	783 K	$4.36 \pm 0.05$ kJ/mol
	Step 3	850 K	$8.41 \pm 0.11$ kJ/mol

### 3.6. Flame Temperature

The flame temperature curves from the thermocouples at three different positions are presented in Figure 7, illustrating which exhibited strong correlations with the TG curves. Taking the PI/PVDF mixture as an example, the TG and flame temperature curves showed three stages. Therefore, the different temperature peaks of polymer combustion likely corresponded to the different decomposition stages.

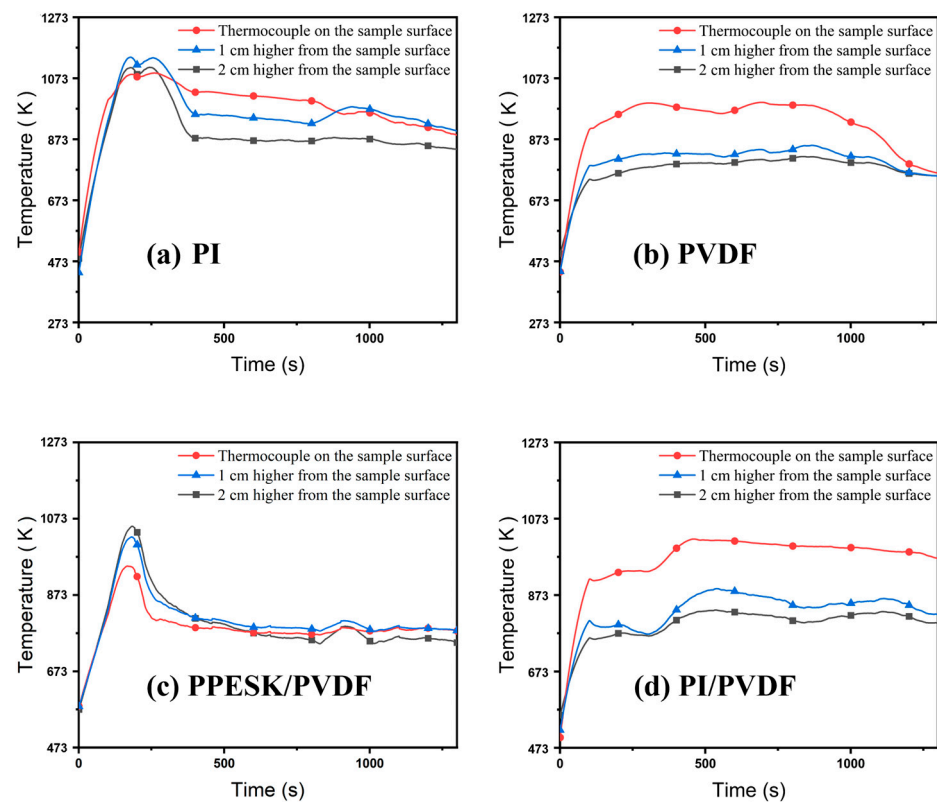


**Figure 7.** Temperature curves of (a) PI, (b) PVDF, (c) PPESK/PVDF, and (d) PI/PVDF during polymer powder combustion using cone calorimetry.

#### 4. Conclusions

In this study, the combustion characteristics of PI, PPESK, PVDF, and the PPESK/PVDF (1:1, mole ratio) and PI/PVDF (1:1, mole ratio) mixtures were studied by cone calorimetry. The main conclusions are as follows,

- According to the combustion index of the polymers and various quantitative parameters, the fire risk of the three single polymer samples was ranked as PPESK > PI > PVDF, and that of the mixtures was ranked as PI/PVDF > PPESK/PVDF. Moreover, the thermal hazard of the polymer materials would be significantly influenced by changes in the external heat flux.
- The HRR curves of the polymer separator materials were consistent with the CO<sub>2</sub> concentration curves. The temperature of the fire could be inferred by measuring the CO<sub>2</sub> concentration. Nevertheless, in the early stage of most fires, the probability of smoke poisoning was higher, while in the stable combustion period, suffocation and burns were more likely to occur.
- After the polymers were mixed, the positive feedback of the two substances in the burning process would change the combustion characteristics of mixtures and could be distinguished from the single polymer. For instance, the pHRR of PI/PVDF was approximately ten times that of PI or PVDF combustion, while for PPESK/PVDF, the pHRR values were between those of PPESK and PVDF, indicating that changes in the combustion characteristics were significantly associated with the polymer materials. Compared with the current commercial PVDF, PPESK and PI are recognized as excellent separator materials with high-temperature resistance. However, according to the results of the present study, in the event of a fire, the addition of PPESK and PI may significantly improve the pHRR. Hence, their combination as separator materials warrants further evaluation.
- According to the fire risk coefficient and activation energy calculated by the Broido method, mixing polymers increases the fire risk. The specific increase depends primarily on the type of mixed polymer components. Therefore, from the point of view of fire suppression, once TR occurs, the addition of PI, or other high-temperature resistant polymers, as separator materials might require more fire extinguishing agents, which has greater firefighting value.

**Author Contributions:** Formal analysis, validation, writing—review & editing, Q.H.; conceptualization, X.L.; investigation, P.H.; data curation, writing—original draft, Y.L.; software, C.L.; funding acquisition, methodology, project administration, Q.C.; resources, supervision, visualization, Q.L. All authors have read and agreed to the published version of the manuscript.

**Funding:** This study has been sponsored by National Key Research and Development Program of China (2021YFB2402003), Tianjin Natural Science Foundation Project (22JCYBJC01690), Key Laboratory of Civil Aviation Thermal Hazards Prevention and Emergency Response (RZH2021-KF-04), National Natural Science Foundation of China (12202410 and 51906238), Project funded by China Postdoctoral Science Foundation (2023T160734 and 2023M733935), Natural Science Foundation of Hunan Province (2023JJ40726), Changsha Municipal Natural Science Foundation (kq2208277), Research Project Supported by Shanxi Scholarship Council of China (2022-139), Natural Science Foundation of Shanxi Province (20210302123017 and 2023 recipient Changcheng Liu), Fund Program for the Scientific Activities of Selected Returned Overseas Professionals in Shanxi Province (20220012) and Supported by the Opening Foundation of Key Laboratory in North University of China (DXMBJJ2023-03). Also, the authors thank Wei Yue and Huifang Zhang from Shiyanjia Lab (<https://www.shiyanjia.com>) for the TG analysis.

**Data Availability Statement:** Data will be made available on request.

**Conflicts of Interest:** The authors declare no conflict of interest.

## References

1. Zhang, Y.; Xia, H.; Lin, J.; Chen, S.; Xu, X. Brief analysis the safety of solid-state lithium ion batteries. *Energy Storage Sci. Technol.* **2018**, *7*, 994–1002. [\[CrossRef\]](#)
2. Jiang, W.; Yu, Y.; Chen, C. A review on lithium-ion batteries safety issues: Existing problems and possible solutions. *Mater. Express* **2012**, *2*, 197–212. [\[CrossRef\]](#)
3. Zhang, M.; Wang, L.; Xu, H.; Song, Y.; He, X. Polyimides as Promising Materials for Lithium-Ion Batteries: A Review. *Nano-Micro Lett.* **2023**, *15*, 135. [\[CrossRef\]](#)
4. Liang, X.; Yang, Y.; Jin, X.; Huang, Z.; Kang, F. The high performances of SiO<sub>2</sub>/Al<sub>2</sub>O<sub>3</sub>-coated electrospun polyimide fibrous separator for lithium-ion battery. *J. Membr. Sci.* **2015**, *493*, 1–7. [\[CrossRef\]](#)
5. Liu, N.; Wu, H.; Mcdowell, M.T.; Yao, Y.; Wang, C.; Cui, Y. A yolk-shell design for stabilized and scalable Li-ion battery alloy anodes. *Nano Lett.* **2012**, *12*, 3315–3321. [\[CrossRef\]](#) [\[PubMed\]](#)
6. Wagemaker, M.; Mulder, F.M. Properties and promises of nanosized insertion materials for Li-ion batteries. *Acc. Chem. Res.* **2012**, *46*, 1206–1215. [\[CrossRef\]](#) [\[PubMed\]](#)
7. Zhong, Y.; Li, J.; Wu, Z.; Guo, X.; Zhong, B.; Sun, S. LiMn<sub>0.5</sub>Fe<sub>0.5</sub>PO<sub>4</sub> solid solution materials synthesized by rheological phase reaction and their excellent electrochemical performances as cathode of lithium ion battery. *J. Power Source* **2013**, *234*, 217–222. [\[CrossRef\]](#)
8. Lu, C.; Qi, W.; Li, L.; Xu, J.; Chen, P.; Xu, R.; Han, L.; Yu, Q. Electrochemical performance and thermal property of electrospun PPESK/PVDF/PPESK composite separator for lithium-ion battery. *J. Appl. Electrochem.* **2013**, *43*, 711–720. [\[CrossRef\]](#)
9. Gong, W.; Wei, S.; Ruan, S.; Shen, C. Electrospun coaxial PPESK/PVDF fibrous membranes with thermal shutdown property used for lithium-ion batteries. *Mater. Lett.* **2019**, *244*, 126–129. [\[CrossRef\]](#)
10. Hermouet, F.; Rogaume, T.; Guillaume, E.; Richard, F.; Marquis, D.; Ponticq, X. Experimental characterization of the reaction-to-fire of an Acrylonitrile-Butadiene-Styrene (ABS) material using controlled atmosphere cone calorimeter. *Fire Saf. J.* **2021**, *121*, 103291. [\[CrossRef\]](#)
11. Meinier, R.; Sonnier, R.; Zavaleta, P.; Suard, S.; Ferry, L. Fire behavior of halogen-free flame retardant electrical cables with the cone calorimeter. *J. Hazard. Mater.* **2018**, *342*, 306–316. [\[CrossRef\]](#)
12. Wang, S.; Ding, H.; Xie, J.; Chen, Y.; Wang, C.; Liu, C.; Huang, Q. A review on the suppression mechanism of typical flame retardants on the explosion of mine dust. *Powder Technol.* **2023**, *427*, 118762. [\[CrossRef\]](#)
13. ISO 5660-1; Reaction-to-Fire Tests—Heat Release, Smoke Production and Mass Loss Rate—Part 1: Heat Release Rate (Cone Calorimeter Method) and Smoke Production Rate (Dynamic Measurement). International Standards Organization: Geneva, Switzerland, 2002.
14. Hohenwarter, D.; Mattausch, H.; Fischer, C.; Berger, M.; Haar, B. Analysis of the Fire Behavior of Polymers (PP, PA 6 and PE-LD) and Their Improvement Using Various Flame Retardants. *Materials* **2020**, *13*, 5756. [\[CrossRef\]](#) [\[PubMed\]](#)
15. Liu, C.; Xu, D.; Weng, J.; Zhou, S.; Li, W.; Wan, Y.; Jiang, S.; Zhou, D.; Wang, J.; Huang, Q. Phase change materials application in battery thermal management system: A review. *Materials* **2020**, *13*, 4622. [\[CrossRef\]](#) [\[PubMed\]](#)
16. Qian, C.; Ding, H.; Xie, J.; Jiang, X.; Chen, Q.; Chen, Y.; Liu, C.; Huang, Q. A review on the transport law and control method of fire smoke from energy storage system in tunnels. *J. Energy Storage* **2023**, *73*, 108929. [\[CrossRef\]](#)
17. Huang, Q.; Wang, S.; He, J.; Xu, D.; Abdou, S.N.; Ibrahim, M.M.; Sun, S.; Chen, Y.; Li, H.; Xu, B.B.; et al. Experimental design of paraffin/methylated melamine-formaldehyde microencapsulated composite phase change material and the application in battery thermal management system. *J. Mater. Sci. Technol.* **2023**, *169*, 124–136. [\[CrossRef\]](#)
18. Huang, Q.; Liu, C.; Wei, R.; Wang, J. Experimental study of polyethylene pyrolysis and combustion over HZSM-5, HUSY, and MCM-41. *J. Hazard. Mater.* **2017**, *333*, 10–22. [\[CrossRef\]](#)
19. Quintiere, J.G. The application of flame spread theory to predict material performance. *J. Res. Natl. Bur. Stand.* **1988**, *93*, 61. [\[CrossRef\]](#)
20. Zhang, Y.; Ji, J.; Wang, Q.; Huang, X.; Wang, Q.; Sun, J. Prediction of the critical condition for flame acceleration over wood surface with different sample orientations. *Combust. Flame* **2012**, *159*, 2999–3002. [\[CrossRef\]](#)
21. Parthasarathy, P.; Anabel, F.; Tareq, A.-A.; Mackey, H.R.; Rosa, R.; Gordon, M. Thermal degradation characteristics and gasification kinetics of camel manure using thermogravimetric analysis. *J. Environ. Manag.* **2021**, *287*, 112345. [\[CrossRef\]](#)
22. Zheng, G.; Wichman, I.S.; Bénard, A. Opposed-flow ignition and flame spread over melting polymers with Navier-Stokes gas flow. *Combust. Theory Model.* **2002**, *6*, 317–337. [\[CrossRef\]](#)
23. Zheng, G.; Wichman, I.S.; Bénard, A. Opposed-flow flame spread over polymeric materials: Influence of phase change. *Combust. Flame* **2001**, *124*, 387–408. [\[CrossRef\]](#)
24. Kim, Y.; Hossain, A.; Nakamura, Y. Numerical modeling of melting and dripping process of polymeric material subjected to moving heat flux: Prediction of drop time. *Proc. Combust. Inst.* **2015**, *35*, 2555–2562. [\[CrossRef\]](#)
25. Wen, C.; Zhang, J.; Levendis, Y.A.; Delichatsios, M.A. A method to assess downward flame spread and dripping characteristics of fire-retardant polymer composites. *Fire Mater.* **2018**, *42*, 347–357. [\[CrossRef\]](#)
26. Broido, A. A simple, sensitive graphical method of treating thermogravimetric analysis data. *J. Polym. Sci. Part A2 Polym. Phys.* **1969**, *7*, 1761–1773. [\[CrossRef\]](#)



27. Gachot, G.; Ribière, P.; Mathiron, D.; Grugeon, S.; Armand, M.; Leriche, J.-B.; Pilard, S.; Laruelle, S. Gas Chromatography/Mass Spectrometry as a Suitable Tool for the Li-Ion Battery Electrolyte Degradation Mechanisms Study. *Anal. Chem.* **2011**, *83*, 478–485. [[CrossRef](#)]
28. Nazaré, S.; Kandola, B.; Horrocks, A.R. Use of cone calorimetry to quantify the burning hazard of apparel fabrics. *Fire Mater.* **2002**, *26*, 191–199. [[CrossRef](#)]
29. Oztekin, E.S.; Crowley, S.B.; Lyon, R.E.; Stoliarov, S.I.; Patel, P.; Hull, T.R. Sources of variability in fire test data: A case study on poly(aryl ether ether ketone) (PEEK). *Combust. Flame* **2012**, *159*, 1720–1731. [[CrossRef](#)]
30. Kashiwagi, T.; Ohlemiller, O.-T. A study of oxygen effects on nonflaming transient gasification of PMMA and PE during thermal irradiation. *Symp. Int. Combust.* **1982**, *19*, 815–823. [[CrossRef](#)]
31. Liu, C.; Huang, Q.; Zheng, K.; Qin, J.; Zhou, D.; Wang, J. Impact of lithium salts on the combustion characteristics of electrolyte under diverse pressures. *Energies* **2020**, *13*, 5373. [[CrossRef](#)]
32. Xu, D.; Huang, G.; Guo, L.; Chen, Y.; Ding, C.; Liu, C. Enhancement of catalytic combustion and thermolysis for treating polyethylene plastic waste. *Adv. Compos. Hybrid Mater.* **2022**, *5*, 113–129. [[CrossRef](#)]
33. Mastori, H.; Sonnier, R.; Ferry, L.; Coutin, M. Fire behavior of lead-containing PMMA based Kyowaglas. *Polym. Degrad. Stab.* **2021**, *190*, 109618. [[CrossRef](#)]
34. Schartel, B.; Bartholmai, M.; Knoll, U. Some comments on the use of cone calorimeter data. *Polym. Degrad. Stab.* **2005**, *88*, 540–547. [[CrossRef](#)]
35. Shi, L.; Michael-Yit-Lin, C. Fire behaviors of polymers under autoignition conditions in a cone calorimeter. *Fire Saf. J.* **2013**, *61*, 243–253. [[CrossRef](#)]
36. Luche, J.; Rogau, T.; Richard, F.; Guillaume, E. Characterization of thermal properties and analysis of combustion behavior of PMMA in a cone calorimeter. *Fire Saf. J.* **2011**, *46*, 451–461. [[CrossRef](#)]
37. Ward, S.-M.; Braslaw, J. Experimental Weight Loss Kinetics of Wood Pyrolysis under Vacuum. *Combust. Flame* **1985**, *61*, 261–269. [[CrossRef](#)]
38. Conesa, J.-A.; Caballero, J.A.; Marcilla, A. Analysis of different kinetic models in the dynamic pyrolysis of cellulose. *Thermochim. Acta* **1995**, *254*, 175–192. [[CrossRef](#)]
39. Qin, J.; Liu, C.; Huang, Q. Simulation on fire emergency evacuation in special subway station based on Pathfinder. *Case Stud. Therm. Eng.* **2020**, *21*, 100677. [[CrossRef](#)]
40. Li, D.; Hu, J.; Wang, C.; Guo, L.; Zhou, J. Metal-organic framework-induced edge-riched growth of layered Bi<sub>2</sub>Se<sub>3</sub> towards ultrafast Na-ion storage. *J. Power Source* **2023**, *555*, 232387. [[CrossRef](#)]
41. Jeske, H.; Arne, S.; Frauke, C. Development of a thermogravimetric analysis (TGA) method for quantitative analysis of wood flour and polypropylene in wood plastic composites (WPC). *Thermochim. Acta* **2012**, *543*, 165–171. [[CrossRef](#)]
42. Wang, X.; Yuan, H.; Lei, S.; Xing, W.; Lu, H.; Lv, P.; Jie, G. Flame retardancy and thermal degradation mechanism of epoxy resin composites based on a DOPO substituted organophosphorus oligomer. *Polymer* **2010**, *51*, 2435–2445. [[CrossRef](#)]

**Disclaimer/Publisher's Note:** The statements, opinions and data contained in all publications are solely those of the individual author(s) and contributor(s) and not of MDPI and/or the editor(s). MDPI and/or the editor(s) disclaim responsibility for any injury to people or property resulting from any ideas, methods, instructions or products referred to in the content.